ResearchGate

See discussions, stats, and author profiles for this publication at: https://www.researchgate.net/publication/241497742

On the role of the CP47 core antenna in the energy transfer and trapping dynamics of Photosystem II

ARTICLE *in* PHYSICAL CHEMISTRY CHEMICAL PHYSICS · OCTOBER 2004

Impact Factor: 4.49 · DOI: 10.1039/b411977k

CITATIONS
36

READS
16

4 AUTHORS, INCLUDING:

Rienk van Grondelle
VU University Amsterdam
647 PUBLICATIONS **23,551** CITATIONS

SEE PROFILE

Jan P Dekker
VU University Amsterdam
175 PUBLICATIONS **8,834** CITATIONS

SEE PROFILE

Available from: Jan P Dekker
Retrieved on: 27 January 2016

RESEARCH PAPER

PCCP
www.rsc.org/pccp

On the role of the CP47 core antenna in the energy transfer and trapping dynamics of Photosystem II

Elena G. Andrizhiyevskaya,* Dmitrij Frolov, Rienk van Grondelle and Jan P. Dekker

Faculty of Sciences, Division of Physics and Astronomy, Vrije Universiteit, De Boelelaan, 1081 HV Amsterdam, the Netherlands. E-mail: elena@nat.vu.nl; Fax: +31 20 4447999; Tel: +31 20 4447935

Received 7th May 2004, Accepted 26th August 2004
First published as an Advance Article on the web 13th September 2004

The CP47–RC complex of photosystem II (PS II) has an antenna subunit of 16 chlorophyll *a* molecules attached to the reaction center (RC) at the side of its inactive branch. The X-ray structure of PS II revealed that the shortest interpigment distances between CP47 and RC are about 21 Å, which is two-three times larger than within each subunit. Such long distances may slow down the energy transfer from CP47 to RC. In order to evaluate the influence of the CP47 antenna on the energy transfer and trapping dynamics in the RC we performed a comparative analysis of CP47–RC and RC complexes from spinach by transient difference absorption and time-resolved fluorescence spectroscopy at room temperature. Our data reveal a complex multiexponential decay of the excited states in both complexes. The main trapping lifetimes are 2–3, 30–40 and 360–460 ps in the RC and 2–6, 80–85 and 650–700 ps in the CP47–RC, the latter two phases being two to three times longer than in the RC. The data could be fitted well with a kinetic model consisting of three reversible radical pair states, the first one being nearly isoenergetic with P680*, and identical energy levels and kinetics of processes occurring within the RC in both complexes. We conclude that there is no kinetic limitation of the energy transfer between CP47 and RC on the two slowest trapping phases and that this transfer occurs in 20 ps or less. The two factors that influence the observed slower trapping in CP47–RC are the highly reversible charge separation reaction in the RC and the presence in CP47 of states with energy lower than the primary electron donor P680.

1 Introduction

In the thylakoid membranes of green plants, algae and cyanobacteria the reaction center (RC) of photosystem II (PS II) is surrounded by a number of pigment-protein complexes that harvest sunlight and efficiently deliver excitation energy to the RC.[1] The subunits most close to the RC are CP43 and CP47, which together with the RC and a number of extrinsic proteins involved in water oxidation constitute the PS II core complex. Structures of cyanobacterial PS II core complexes were obtained recently at 3.5–3.8 Å resolution.[2–4] The main features of the cyanobacterial structure match reasonably well those of green plants, so it is valid to use the X-ray structure of PS II from cyanobacteria as a model for the structure of the PS II core complex of higher plants.[5]

According to the X-ray structure the RC (D1/D2/Cyt b_{559}) complex comprises 8 chlorins and 2 carotenes, all of which participate in the energy transfer and/or electron transfer processes. Four chlorophyll (Chl) and two pheophytin (Pheo) molecules are arranged in two branches in the central part of the complex. One branch is known to be active in charge separation.[9] Two Chl molecules are bound at the periphery of the complex at distances of about 24 Å from the core pigments and do not participate in the primary charge separation process, though they can be involved in secondary electron transfer processes, just as the two β-carotene molecules and cytochrome b_{559}.[6]

The CP47 complex contains 16 Chls and two β-carotenes.[4] In the thylakoid membrane it is located at the side of the inactive branch of the RC. The closest interpigment distance between CP47 (Chl43 according to the nomenclature in ref. 2) and RC ($Pheo_{D2}$ and $ChlZ_{D2}$) is about 21 Å, which is considerably more than the *ca.* 9 Å average interpigment distance in CP47.

In all PS II RC preparations obtained thusfar the secondary electron acceptors, the plastoquinones Q_A and Q_B, were removed from their binding sites during the isolation procedure, implying that photochemistry does not proceed beyond the primary radical pair. The CP47–RC complex differs from the RC mainly by the presence of the additional antenna subunit, because Q_A is also largely absent after isolation and purification.[7] This means that these two complexes represent a good target for comparative studies of the influence the CP47 core antenna on the energy transfer and charge separation processes in the RC.

The kinetics of energy transfer and trapping in the RC have been studied by several groups using both ultrafast absorbance difference and fluorescence techniques. The results were reviewed elsewhere.[8,9] According to these studies the transfer of excitation energy within the six central chlorins of the RC is ultrafast, with a time constant of about 100 or 600 fs upon excitation into the blue or red edge of the Q_y absorption band, respectively,[10] though slower energy transfer components can probably not be excluded, in particular at low temperatures.[11] It was suggested[12] that charge separation occurs from an excited state which at least at room temperature is distributed over a significant fraction of the six core chlorins, depending on the particular realisation of the disorder. The charge separation reactions are strongly multiphasic, with main components in the range of 0.4–3, 20–50 and 120–500 ps. The details of charge separation process are not precisely understood yet, especially with regard to the role of the "accessory" Chl on the active branch of the RC (Chl_{D1} according to the nomenclature in ref. 2). It has been proposed that at least at low temperatures Chl_{D1} acts as primary electron donor and that the Chl_{D1}^{+} $Pheo_{D1}^{-}$ pair occurs first, followed by electron transfer from P_{D1} to Chl_{D1}^{+}.[13] The findings that Chl_{D1} is the red-most absorbing

DOI: 10.1039/b411977k

 This journal is © The Owner Societies 2004

chromophore in the PS II RC[14] and that $Pheo_{D1}$ and Chl_{D1} give rise to a charge-transfer state of about equal energy with those of the main exciton states[15] are in line with this idea.

Lifetimes of about 0.4, 3 and 8 ps were suggested for the primary charge separation.[8,9] The 20–50 ps processes were interpreted as formation of a secondary radical pair or primary charge separation limited by the slow transfer from the peripheral Chls to the core of RC.[16–20] The 200–500 ps kinetics, initially attributed to radical pair relaxation due to electron transfer to Q_A,[21] were also observed in isolated RC preparations, which do not contain Q_A.[22] It was proposed that the slow relaxation reactions of the radical pair may be induced by conformational changes of the protein, induced by the creation of the two charges.[23]

Recent experiments indicated that most of the energy transfer dynamics in CP47 occurs within 2–3 ps.[24] In CP47 the lowest energetic state absorbs at 690 nm with an oscillator strength equal to that of 1 Chl. The 690 nm state gives a major contribution to the low temperature emission of CP47 and determines a 17 ps lifetime of energy transfer in CP47 at 77 K. The 690 nm pigment is most probably located at the periphery of CP47 not close to the RC and its population will slow down rather than speed up the energy transfer to the reaction center.[25]

For PS II core complexes it was initially proposed[21,26] that excitation energy equilibrates rapidly within several hundreds of femtoseconds between the core antenna and the RC, and that then charge separation occurs within several picoseconds (trap-limited model). Earlier fluorescence measurements performed on CP47–RC and larger PS II particles[27,28] supported the fast energy equilibration between core antenna and RC.

In contrast, calculations of energy transfer rates[29] performed on the basis of the recently published PS II structures suggested slow energy transfer from the core antenna to RC, even though most of the Chls in the core antenna are oriented in a way favourable for efficient transfer to the RC.[30] The lifetime of charge separation depends in this case on the slow energy delivery process from the core antenna to the RC (transfer-to-the-trap-limited model).

In this contribution we present room temperature transient absorption and time-resolved fluorescence studies on PS II RC and CP47–RC complexes purified from spinach. Our goal was to record the energy transfer and trapping processes in RC and CP47–RC under similar experimental conditions to be able to make a reliable comparison of the obtained results. The results indicate that the presence of the CP47 antenna reduces the rate constants of trapping by a factor of 2–3. A fit based on a kinetic model suggests that the slower trapping observed in CP47–RC is caused by a shift of the excited states distribution towards the CP47 antenna, and that the intrinsic rate for energy transfer from CP47 to RC does not limit the overall trapping kinetics in the CP47–RC complex.

2 Materials and methods

2.1 Sample preparation

PSII RCs were purified from spinach Tris-washed "BBY" grana membranes[31] as described by van Leeuwen *et al.*[32] CP47–RC complexes were purified from spinach as described elsewhere.[7]

For the spectroscopic measurements, all samples were diluted in a buffer containing 20 mM Bis-Tris (pH 6.5), 10 mM $MgCl_2$, 10 mM $CaCl_2$ and 0.03% *n*-dodecyl-β-D-maltoside (β-DM). Semi-anaerobic conditions in the samples were created by addition of catalase, glucose and glucose oxidase, in that order, to final concentrations of 120 μg ml^{-1}, 10 mM and 120 μg ml^{-1}, respectively. The optical density (OD) of the samples used for the transient absorption and fluorescence measurements was about 0.7 mm^{-1} and 0.8 cm^{-1}, respectively, at the Q_y absorption maximum. The steady state absorption of the samples was compared before and after measurement. Sample degradation was in all cases less than 1%. We also analyzed the CP47–RC complex before and after measurement by diode-array-assisted gel filtration chromatography[33]. This technique allows a quantitative estimation of the amount of free CP47 and free pigments in the samples. The results revealed a contamination of free CP47 complexes of 1% or less in the samples and no measurable amount of free chlorophylls (not shown), suggesting no significant contribution of unbound CP47 or free chlorophylls to the observed kinetics.

2.2 Transient absorption

Absorption difference spectra were recorded with a femtosecond spectrophotometer, described in detail elsewhere.[34] In brief, the output of Ti:Sapphire oscillator (Coherent Mira) was amplified by means of chirped pulse amplification (Alpha-1000 US, B. M. Industries), generating 1 kHz, 800 nm, 60 fs pulses. Single-filament probe white light was generated in a 2 mm sapphire plate. Pump light at 400 nm was obtained by doubling the 800 nm fundamental *via* a SHG crystal. Pump light in the visible wavelength range was produced in a home-built, non-collinear optical parametric amplifier. After prism compression, the pulse duration was reduced to 50–60 fs. Interference filters with transmission maxima at 662 and 695 nm and fwhm 12 and 15 nm, respectively, were used to select the wavelength of excitation. Transient absorption difference spectra were collected with probe and excitation beams oriented at magic angle. The excitation beam was focused in a spot with 350 μm diameter. The energy of excitation was 15 nJ $pulse^{-1}$ upon 662 and 695 nm excitations, and 30 nJ $pulse^{-1}$ upon 400 nm excitation. We estimated that about 0.25–0.5 photons were absorbed by each complex per laser shot upon 400 nm excitation, and 0.1–0.2 photons per complex upon 662 and 695 nm excitations. The cuvette (1 mm pathlength) was shaken in order to refresh the sample from shot to shot. The time resolution was typically 120 fs and the spectral resolution was 3 nm. The data were corrected for white light group velocity dispersion and instrument response, and fitted globally as described in ref. 35. A coherent coupling between pump and probe pulses[36,37] was included into the fit function for the data obtained upon 662 and 695 nm excitations.

2.3 Time-resolved emission

Time-resolved fluorescence emission spectra were recorded with a Hamamatsu C5680 synchroscan streak camera as described in ref. 38. In short, the output of a Ti:Sapphire oscillator (Coherent Mira-Rega), generating 125 kHz, 800 nm, 150 fs pulses, was doubled *via* an OPA (Coherent), producing 125 kHz, 400 nm, 150 fs pulses. A 665 nm light was generated *via* the OPA (Coherent) and selected with the interference filter with fwhm = 5 nm. The sample was placed in a spinning cell (diameter 10 cm) with rotation frequency of 75 Hz. The excitation energy was 1–2 nJ/pulse and the excitation beam was focused in a spot with 150 μm diameter, corresponding to about 0.05–0.1 absorbed photons per complex. Fluorescence was collected at magic angle with respect to the polarization of the excitation beam. The time resolution was 3.5 ps for 400 nm excitation and 6 ps for 665 nm excitation, the spectral resolution was 5 nm. The fluorescence data were corrected for white light group velocity dispersion and instrument response, and fitted globally as described in ref. 38.

3 Results

3.1 Steady-state absorption

Fig. 1 shows room temperature absorption spectra of the isolated RC and CP47–RC complexes. The Q_y absorption

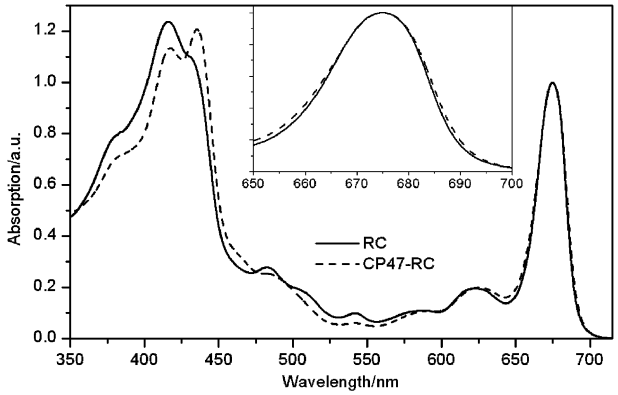

Fig. 1 Room temperature absorption of the RC and CP47–RC complexes.

band peaks at 675 and 675.5 nm for the RC and CP47–RC respectively. The Q_y absorption band of the RC is highly congested, though there is some evidence that the peripheral Chls contribute more to the blue side of the Q_y absorption (670–675 nm),[17,39] and that most of the six central chlorins of the PS II RC absorb at around 680 nm.[40] Thus, some selectivity can be achieved upon applying different wavelengths of excitations. The Q_y band of isolated CP47 overlaps fully with that of the PS II RC and is even broader than this spectrum due to the presence in CP47 of Chls absorbing at energies higher and lower than those of the RC. Thus selective excitation of one of subunits within CP47–RC can not be achieved. The different lineshapes of the two preparations in the Soret region is explained by the relatively higher content in the RC of Pheo *a* and cytochrome *b*-559, which both have strong absorbances at 416 nm.[33]

3.2 Transient absorption

Transient difference absorption spectra of RC and CP47–RC were measured on a time scale up to 4 ns upon excitation into the Soret band of Chl *a* (λ_{ex} = 400 nm), and the blue and red edges of the Q_y absorption band (λ_{ex} = 662 and 695 nm, respectively). The decay-associated difference spectra (DADS) obtained after global analysis are shown in Fig. 2.

RC. The decay of delta absorption in the PS II RC complex could be fitted reasonably well with five components for 662 and 400 nm excitation and three components for 695 nm excitation.

The first DADS has a lifetime of about 100 fs and has a very different shape for the three wavelengths of excitation. Upon 400 nm excitation it has a strongly positive amplitude (Fig. 2e), indicating that excited states of Q_y absorption bands are populated during this time. This phase can therefore be attributed to Soret to Q_y relaxation processes. The first DADS upon 662 nm excitation (Fig. 2c) has a negative peak at 670 nm and a positive peak at 683 nm. The conservative shape suggests energy transfer from species absorbing maximally at 670 nm to species absorbing maximally at 683 nm. Subpicosecond equilibration processes in PS II RC complexes were observed and extensively discussed before.[10] This fast equilibration must almost exclusively occur within the six central chlorines of the PS II RC, because there is evidence that the peripheral Chls transfer energy to the central pigments on a much slower timescale (10–30 ps).

The second DADS has a lifetime of about 2–3 ps and has similar, but not identical shapes upon different wavelengths of excitation. For 400 and 695 nm excitation it consists of a negative band peaking at about 683 nm and a positive band around 660–670 nm. For 662 nm excitation, the negative band is slightly blue-shifted while no positive band between 660 and 670 is observed. We attribute this phase to primary charge separation. Merry *et al.*[10] reported a 600 fs uphill energy transfer in PS II RC complexes upon 694 nm excitation, which was better resolved in data with a parallel orientation of pump and probe beams. It is possible that uphill energy transfer contributes to the 2 ps DADS in our magic angle data upon 695 nm excitation, but that it could not be resolved as a separate, 600 fs component. The shape of the 2 ps DADS obtained upon 400 and 695 nm is similar to the 3 ± 1 ps DADS obtained upon 543 nm excitation into the Q_x band of Pheo *a* (data not shown). This gives evidence that Pheo contributes to the absorption around 680 nm and also confirms that Pheo participates in the initial charge separation process.

The third DADS has a lifetime of about 20–30 ps and has a negative amplitude in the whole Q_y range, except for a positive feature around 680 nm upon 662 and 400 nm excitation. The negative contribution in the red edge of this DADS for a large part is due to the decay of stimulated emission. Stimulated emission must occur from excited states, implying that excited states still contribute to the observed absorption changes on the tens of ps timescale, in line with the fluorescence measurements (see below). The positive feature around 680 nm may occur as a result of several processes: energy transfer from peripheral chlorophylls peaking at 670 nm, electrochromic bandshifts caused by the positive and negative charges associated with P_{D1}^+ $Pheo_{D1}^-$ formation, like in the bacterial RC,[41] and a blueshift of red exciton states caused by P_{D1}^+ $Pheo_{D1}^-$ formation. Excitation at 695 nm will prevent the first possibility, and the absence of the positive 680 nm feature upon 695 nm excitation suggests that energy transfer from peripheral chlorophylls at 670–680 nm states gives an important contribution to the overall kinetics.

The fourth DADS has a very small amplitude in transient absorption, and has a lifetime of about 360–460 ps. This phase was not observed upon 695 nm excitation, which could be due to its small amplitude. This phase has a prominent amplitude in the fluorescence decay (see below), and can therefore be attributed to radical pair relaxation.

The non-decaying (ND) absorbance within the time range of our experiments has a minimum at 680 nm and is positive at wavelengths longer than 700 nm, which is an indicator of presence of the $P_{D1}^+Pheo_{D1}^-$ radical pair, the final product of charge separation.[18] It is known that in the isolated RC the radical pair has a lifetime of about 50 ns at room temperature,[42] which then recombines to the ground state or the P680* singlet or triplet state. Its shape is identical upon all wavelengths of excitation.

CP47–RC. The global analysis revealed six, five and four components for CP47–RC upon 400, 662 and 695 nm excitation (Fig. 2b, d, f). The first DADS (80–180 fs) have similar shapes as those observed in the RC and similar origins: Soret to Q_y energy transfer for 400 nm excitation and energy equilibration between 670 and 680 nm absorbing species for 662 nm excitation. It is likely that the latter phase occurs not only in the RC, but also within CP47, because in isolated CP47 a strong 200 fs energy transfer from 670 to 680 nm absorbing species was found (at 77 K).[24]

In all traces one or two transients were found with lifetimes of 2–6 ps. These lifetimes most probably reflect a mixture of at least two processes: downhill energy transfer within CP47, as was shown to occur at 77 K,[24] and charge separation within the RC (like the 2.5 ps component in the RC). It is also possible that energy equilibration between CP47 and RC contributes to this phase. The shapes of the 2–4 ps phases are similar to those of the corresponding phases in the RC, which suggests that direct charge separation within the RC contributes to a significant extent to these phases. The 6 ps phase upon 400 nm

 This journal is © The Owner Societies 2004

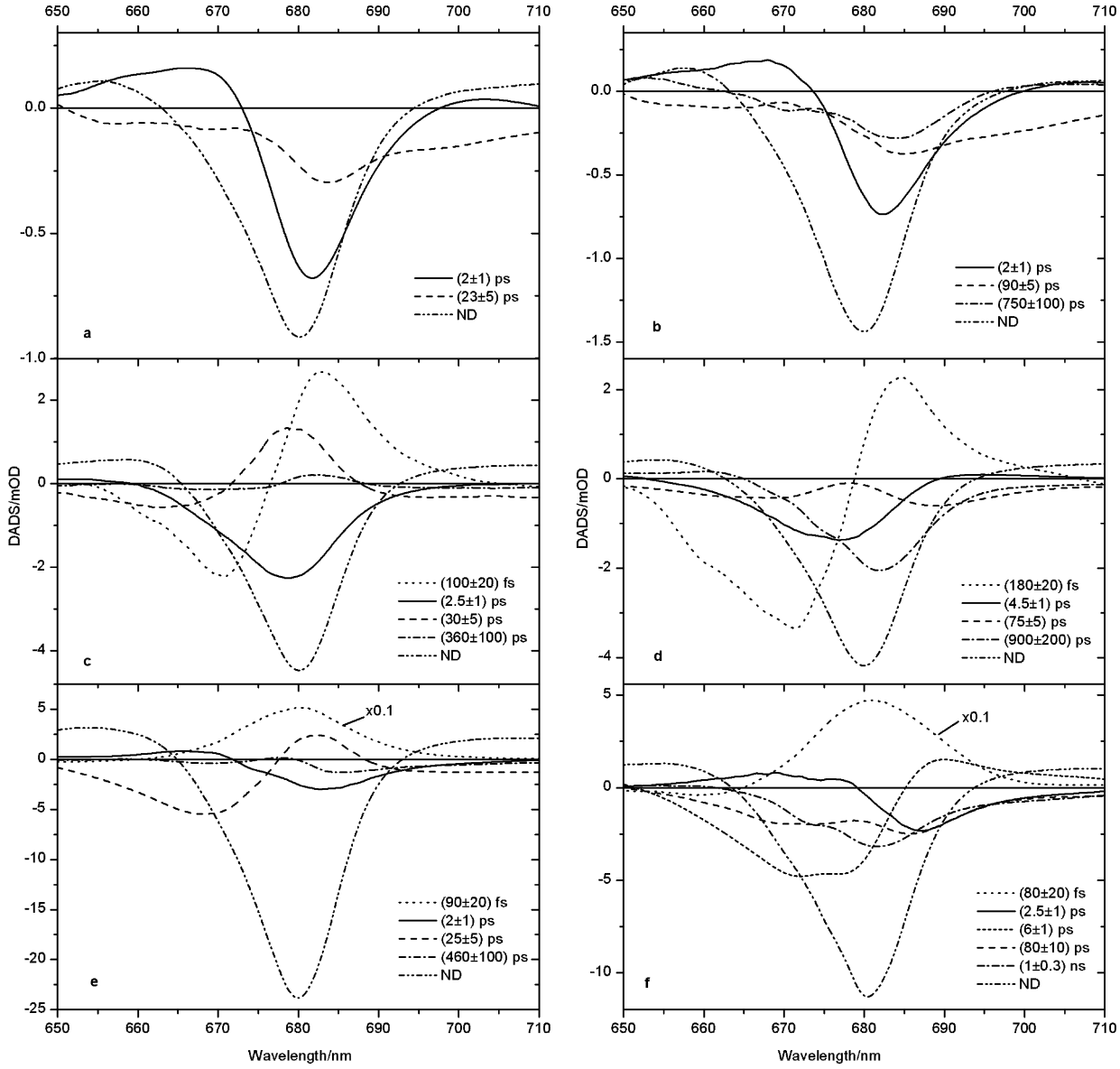

Fig. 2 DADS of RC (a),(c),(e) and CP47–RC (b),(d),(f) upon 695 nm (a),(b), 662 nm (c),(d) and 400 nm (e),(f) wavelengths of excitation.

excitation has a shape consistent with downhill energy transfer within CP47.

The third series of DADS have lifetimes of 75–90 ps and have roughly similar shapes as those of the 20–30 ps DADS in the RC, exept for the large negative feature caused by CP47 excited states. The negative amplitudes suggest that they all reflect a recovery of bleach, caused by a conversion of chlorophyll/pheophytin excited states into their oxidizes/reduced states. These DADS can therefore be attributed to the secondary trapping process, which in CP47–RC has an about threefold increased lifetime.

A fourth series of DADS have lifetimes of 750–1000 ps. The amplitudes of these DADS are larger than those in the RC, and the lifetimes are two to three times longer. It is likely that a third step of radical pair relaxation contributes to these decays. The fact that these DADS are larger than in the RC can be explained by the fact that due to the presence of CP47 about 3x more excited states remain before this phase occurs.

For all excitation wavelengths, the non-decaying (ND) components have similar shapes as those observed for the RC, and thus reflect the absorbance difference spectrum of the P_{D1}^{+} $Pheo_{D1}^{-}$ radical pair.

From the results of this section we conclude that in both complexes multiexponential trapping by charge separation occurs. The lifetimes of trapping are about 2–3, 23–30 and 360–460 ps for the RC and 2–4, 70–90 and 700–1000 ps for CP47–RC. The last two processes are about three times longer in CP47–RC than in the RC.

3.3 Steady-state emission

Fig. 3 shows the steady-state emission spectra of RC and CP47–RC at room temperature which peak at 681 and 683 nm, respectively. Isolated CP47 peaks at 683 nm.[44] The 2 nm red shift of the CP47–RC emission maximum is consistent with the fact that CP47 makes a significant contribution to the emission of the CP47–RC complex.

3.4 Time-resolved emission

We have measured time-resolved fluorescence spectra of RC and CP47–RC upon 400 and 665 nm excitation, using a streak camera set-up. This technique allows a better time and spectral resolution than the more commonly used single-photon timing technique, and was used before for an analysis of RC complexes with red excitation (F. van Mourik *et al.*, manuscript in preparation). For our experiments, the time resolution was 3.5 ps for 400 nm excitation and 6 ps for 665 nm excitation. This

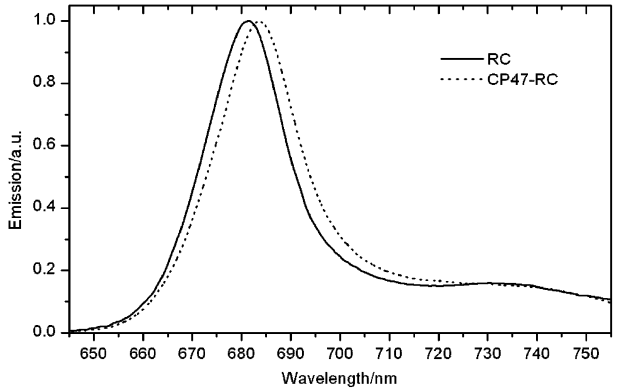

Fig. 3 Room temperature emission of RC and CP47–RC.

was not sufficient to resolve subpicosecond processes with similar accuracy as in pump–probe experiments. Experimental traces are shown in Fig. 4. It is obvious from these pictures that CP47–RC is characterised by a longer decay of the emission than RC. The decay associated emission spectra (DAES) for RC and CP47–RC are shown in Figs. 5 and 6.

RC. Apart from a poorly resolved sub-picosecond transient, four components were needed to fit the fluorescence decay of the RC for 400 and 665 nm excitation (Figs. 5a and 6a, respectively). The first DAES has a lifetime of about 3 ps, and peaks considerably (400 and 695 nm excitation: F. van Mourik *et al*., manuscript in preparation) or slightly (665 nm excitation) more to the red than all subsequent decay phases. The DAES for 400 nm excitation has a positive peak at 690 nm and a small negative feature at 672 nm. The shape of this DAES is non-conservative (with a large positive and a small negative part). The large positive part (decrease of fluorescence) reflects the trapping by charge separation from states emitting around 685–690 nm. The small negative part can be explained by uphill energy transfer.

The following DAES have positive amplitudes and lifetimes of 39 and 360 ps, and reflect subsequent processes of trapping by charge separation. This subsequent trapping could only be observed in fluorescence measurements when excited states are still present in the complex, *i.e*. if trapping is intrinsically multi-exponential. One possible cause for multi-exponentiality is that trapping is reversible and that the initially formed radical pair 'relaxes', which will causes a decrease of excited states population resulting in a decrease of fluorescence. The 39 ps DAES upon 400 nm excitation and the 400 ps DAES upon both excitation wavelengths are similar in shape compared to the steady-state emission of the RC, suggesting that at least the 400 ps processes occur from excited states equilibrated over all pigments. Comparison of the 40 ps DAES upon 400 and 665 nm excitation (Fig. 7) reveals that this DAES upon 665 nm excitation has a larger contribution in the blue part around 670 nm. This suggests that the 40 ps trapping process occurs from a non-equilibrated state and thus can be a mixture of at least two processes: slow energy transfer from (peripheral) chlorophylls absorbing around 670 nm, and trapping by the formation of a secondary radical pair. The 400 ps DAES contributes significantly to the emission of the RC, consistent with radical pair relaxation. The last DAES have a lifetime more than 15 ns which can be attributed to the lifetime of radical pair.

CP47–RC. The DAES obtained for CP47–RC upon 400 and 665 nm excitation are shown in Figs. 5b and 6b, respectively. The first DAES has a lifetime of about 5 ps, but a very different shape for both excitation wavelengths. Upon 665 nm excitation, it has a positive peak at 675 nm and negative peak at 695 nm, consistent with energy transfer within CP47. The non-conservative character of this DAES suggests that trapping also occurs on the same time scale. Upon 400 nm excitation, the shape of this component is similar to the 3 ps component in the RC. Its amplitude, however, is smaller than that of the next DAES in the CP47–RC complex. This phase must be largely due to charge separation.

The following two DAES have positive amplitudes and reflect trapping by charge separation with lifetimes of about 80–85 ps and 650–700 ps. These times are similar to those observed in transient absorption, and the amplitudes suggest that both processes contribute about equally to the trapping. The large amplitudes of these DAESes suggest that the decay of CP47 excited states largely contributes to these components. The last DAES has a lifetime longer than 15 ns which can attributed to the lifetime of radical pair.

4 Kinetic model

The analysis of the time-resolved fluorescence and transient difference absorption data allowed us to make the following conclusions. In the PS II RC complex, the excitation energy is rapidly (about 100 fs and less than 2–3 ps upon excitation in the blue and red edges of the Q_y absorption band, respectively) redistributed among the central six pigments of the RC between states absorbing at around 670 and 680 nm. Then the initial trapping process occurs with a timeconstant of 2–3 ps. The following 30–40 ps process is a mixture of at least two: secondary radical pair formation and transfer of excitation energy from blue-shifted Chls. A 360–460 ps trapping phase can be assigned to further radical pair relaxation. The relaxed radical pair lives longer than 15 ns.

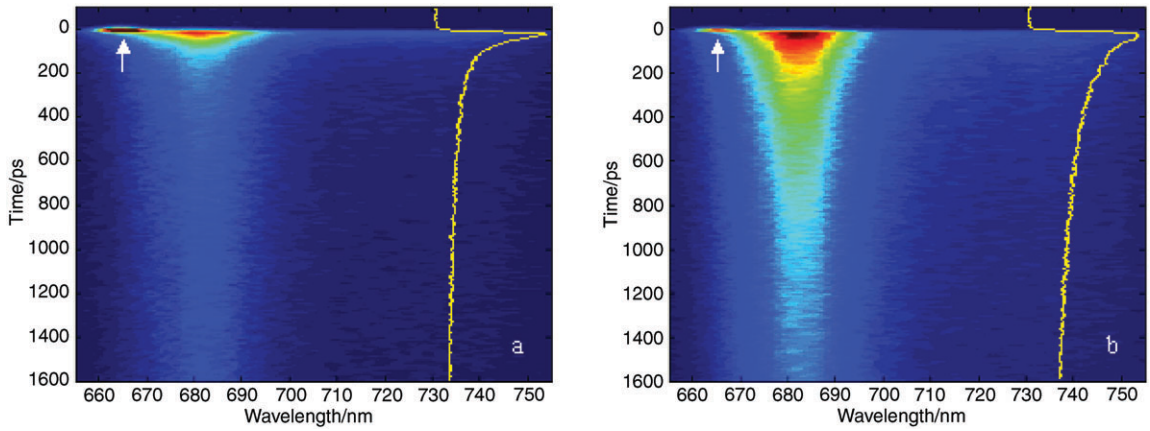

Fig. 4 2D images of emission data for the RC (a) and CP47–RC (b) upon 665 nm excitation. Arrows indicate Rayleigh scattering of the excitation beam. The yellow lines are data profiles taken at 682 nm.

This journal is © The Owner Societies 2004

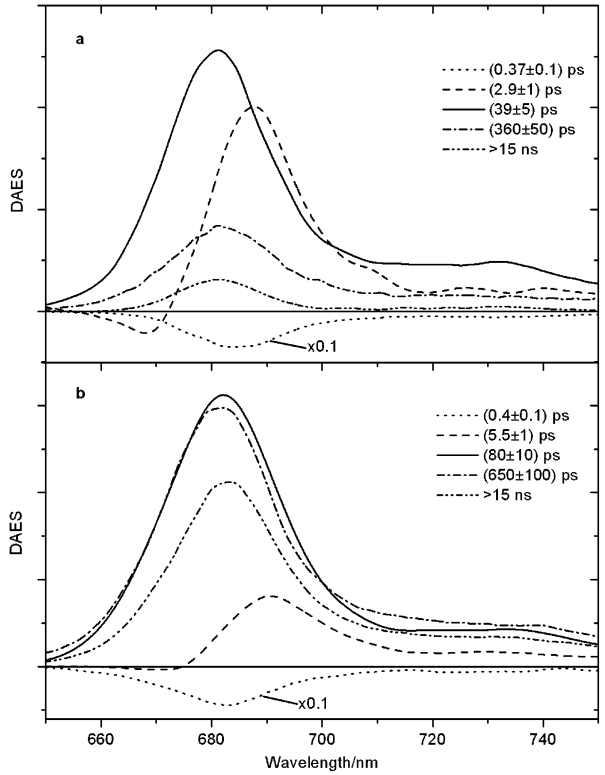

Fig. 5 DAES upon 400 nm excitation for RC (a) and CP47–RC (b).

In CP47–RC, the first trapping phase takes place on the 2–6 ps timescale, but its kinetics can not easily be followed because of the presence of a major energy transfer process within CP47 in the same time range. Also energy transfer between CP47 and RC can in principle occur on this timescale. Just as in the RC there are two subsequent trapping phases. Both are about three times longer in CP47–RC than in RC. Thus, the addition of the CP47 antenna results in a lengthening of the two slow phases in excited state decay by a factor of about three.

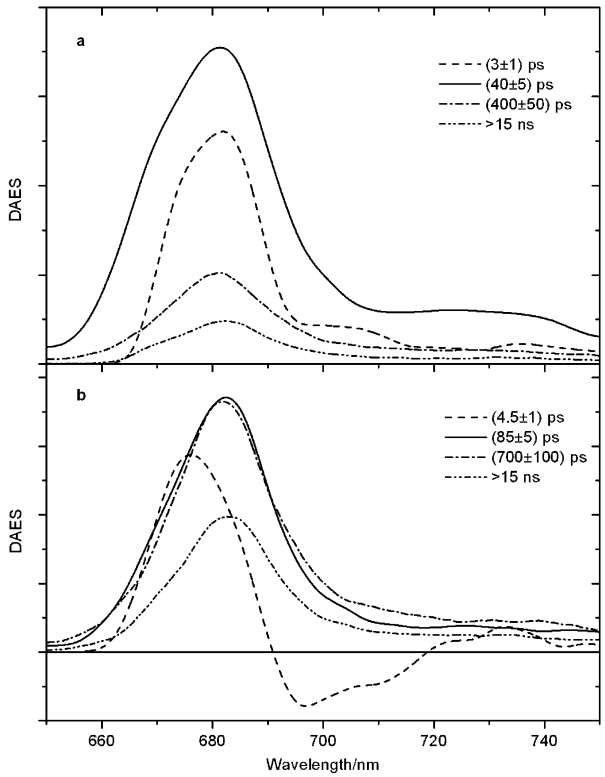

Fig. 6 DAES upon 665 nm excitation for RC (a) and CP47–RC (b).

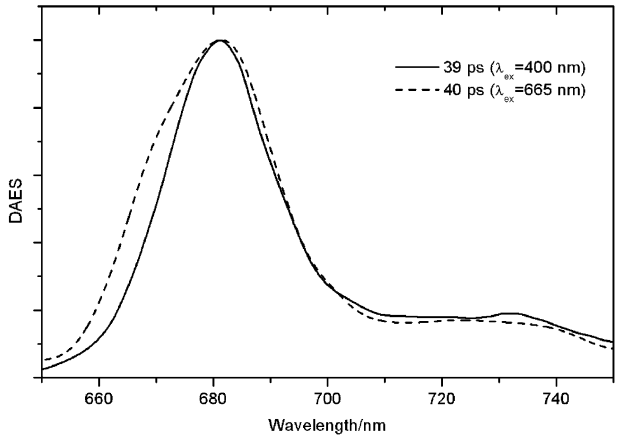

Fig. 7 The 39 and 40 ps DAES for RC upon 400 and 665 nm excitation.

These experimental observations can be explained in at least two ways: (1) the intrinsic rate constant of energy transfer between CP47 and RC is slow due to long distances between the pigments of CP47 and RC; this slow transfer would slow down the subsequent process of trapping in the RC, and (2) the intrinsic rate constant of energy transfer between CP47 and RC is fast, while the excited states distribution is shifted towards CP47 because of red-absorbing states. The equilibration of the excited states over a larger antenna will then cause the slower trapping lifetimes observed in the experiments. These two possibilities can be summarized as transfer-to-the-trap-limited and trap-limited kinetics, respectively.

For the RC, we used a model with five compartments (Fig. 8a). Compartments 'A*' and 'RC*' correspond to the average excited state energy levels of blue 670 Chls and bulk 680 chlorins, respectively. The former may correspond to the two distant Chls in the RC; the latter to the six central chlorins of the RC core. Compartment 'RP1' represents the energy level of the first radical pair. The subsequent relaxations of the radical pair are represented by the compartments 'RP2' and 'RP3'. For simplicity, we discard fast equilibration within the RC core, and thus assume that charge separation takes place from a state equilibrated over all core pigments. We only modelled the fluorescence data upon 665 nm excitation. All compartments are connected by forward and backward energy transfer. The back transfer rate was calculated *via* the Boltzmann factor: $k_{ji} = k_{ij}(N_i/N_j)\exp(-\Delta_{ij}/kT)$, in which N_i is the number of chlorophylls in compartment i, Δ_{ij} is the energy difference between compartment i and compartment j, k is Boltzmann's constant, T is the absolute temperature. The losses including emission are expressed *via* the value k_{fl}^{-1} which is of the order of the lifetime of fluorescence of free Chl. The total emission decay is proportional to the sum of decays of populations of excited states 'A*' and 'RC*'.

In order to exclude the influence of apparatus response functions on the experimentally measured kinetics, we used data obtained from global analysis of the fluorescence measurements, and integrated over all wavelengths. The latter simplification is justified, because apart from the 2–3 ps phase all decay components have similar spectra. The model presented in Fig. 8a gives a good fit of the fluorescence decay in the PS II RC. The fit for the 665 nm excitation data is shown in Fig. 9a. The parameters of the fit are listed in Table 1 together with the reciprocal eigenvalues obtained from the solution of the master equation describing the model. The reciprocal eigenvalues are close to the time constants obtained in the experiment. Values of 25.7 and 37.4 ps can not be resolved separately, and give a single value of 23–30 ps in pump–probe and 39 ps in fluorescence. The energy gap between 'A*' and 'RC*' is 284 cm^{-1}, assuming that blue Chls and bulk chlorins

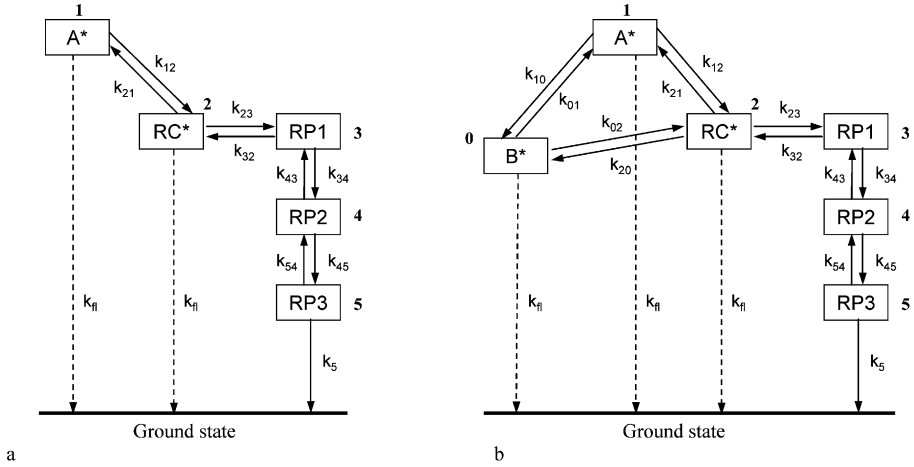

Fig. 8 Compartment model for the RC (a) and CP47–RC (b).

absorb maximally at 670 and 683 nm respectively. Slight changes in these energy levels did not significantly influence the fit. We assumed that 'RC*' and 'RP1' are nearly isoenergetic. Slightly higher or lower energy levels for 'RP1' relatively to 'RC*' did not increase the quality of the fit. The two subsequent relaxations give an energy differences between 'RC*' and the final charge separated state 'RP3' of 76.5 meV. This value has been measured to lie between 46 and 110 meV.[23,43–46] The fact that the initial radical pairs are not much below the excited state in free energy explains why the emission can be observed over such a long time window. The contribution of each compartment of the model to the total decay of emission is shown in Fig. 10a. It is clear from the picture that 'RC*' and 'RP1' fully equilibrate in about 180 ps. After that the populations of the both states remain similar. The contribution of the blue chls (compartment 'A*') to the total decay is essential only up to about 100 ps.

For the CP47–RC we added an additional compartment 'B*' (Fig. 8b) corresponding to the average energy level of CP47. 'B*' is reversibly connected with the compartments 'A*' and 'RC*'. In this case compartment 'A*' corresponds to the average energy level of only one distant Chl from RC, the closest to CP47. The total emission decay is proportional to the sum of decays of populations of excited states 'A*', 'B*' and 'RC*'. The fit of CP47–RC fluorescence upon 665 nm excitation is shown in Fig. 9b. For the processes occurring within the RC, we used the same energy levels and rate constants as found for the isolated RC complex. The parameters of the fit and the eigenvalues are listed in Table 2. To obtain a good fit of the experimental data it was necessary to set level 'B*' lower in energy than 'RC*'. A small energy gap of 42.9 cm^{-1} (see Table 2) still allows efficient uphill energy transfer from 'B*' to 'RC*' at room temperature. Furthermore, a good fit of the data can only be obtained if the intrinsic rate constant of energy transfer from CP47 to RC is sufficiently fast. We found an upper limit for this transfer rate of $(20\ ps)^{-1}$. Slower rates result in a too slow decay of the excited states, which can only be corrected for by changing the energy levels of the secondary and tertiary radical pairs in the RC. The contribution of each compartment to the total decay of the emission is shown in Fig. 10b. The ingrowth of population of each radical pair in CP47–RC is now much slower than in RC, which is because the excited states distribution is shifted towards CP47.

The main conclusion of this section is that good fits of the excited state decay can be obtained by a reversible radical pair model coupled to two subsequent relaxed radical pair states. If the energy levels of the three radical pairs do not change as a result of the addition of CP47, then the energy transfer between CP47 and RC does not limit the overall kinetics. The slowing down of the trapping kinetics upon the addition of CP47 is explained by a shift of the excited state distribution towards CP47.

5 Discussion

5.1 RC

The analysis of transient difference absorption and time-resolved emission data revealed a multiexponential decay of the excited states in the PS II RC. Typical trapping lifetimes in the RC are 2–3, 30–40 and 350–450 ps. Multiexponential trapping in the PS II RC was also observed in earlier experiments, as

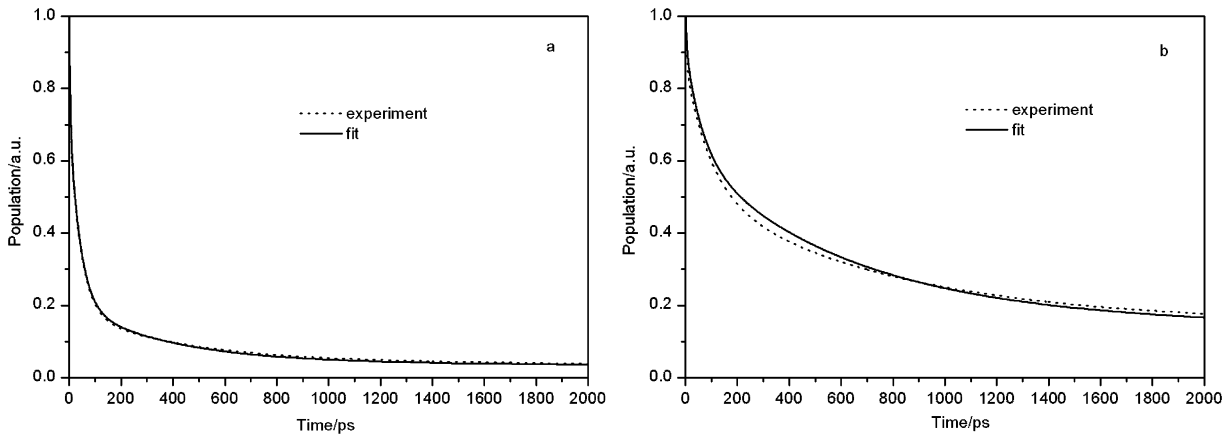

Fig. 9 Integrated decay of emission and fit obtained on the basis of the compartmental model for the RC (a) and CP47–RC (b).

 This journal is © The Owner Societies 2004

Table 1 Parameters of the compartment model for the RC[a]

Δ_{12}/cm^{-1}	Δ_{23}/cm^{-1}	Δ_{34}/cm^{-1}	Δ_{45}/cm^{-1}	k_{12}^{-1}/ps	k_{21}^{-1}/ps	k_{23}^{-1}/ps	k_{32}^{-1}/ps	k_{34}^{-1}/ps	k_{43}^{-1}/ps	k_{45}^{-1}/ps	k_{54}^{-1}/ps	k_5^{-1}/ps	k_{fl}^{-1}/ps
262.6	0	294.9	322	30	326.8	7	7	23	97.9	320	1562	15000	5000

[a] The reciprocal eigenvalues: 3.2 ps; 25.4 ps; 37.8 ps; 373.6 ps; 16.9 ns.

well as in CP47–RC (this work) and PS II core preparations.[47] Initially it was thought that the wide spread of trapping times is due to sample heterogeneity and/or to a wide distribution of the free energy difference of radical pair formation. Later it was suggested that radical pair formation induces a reorganization of the protein surroundings, which in turn reduces the energy level of the radical pair.[23] Also secundary electron transfer reactions, e.g., from P_{D1} to Chl_{D1}^{+}, may reduce the free energy of the radical pair.

Our data are consistent with the following model. Excitation energy rapidly equilibrates within the six central chlorines of RC. Some or most equilibration takes place in about 100 fs, the remainder within a few ps at most. Then initial charge separation takes place in 2–3 ps. The red shifted position of the 2–3 ps component in the transient absorption (400, 695 and 543 nm excitation) and time-resolved emission (400 and 680 nm excitation) indicates that initial charge separation starts from a red exciton state in the RC. This was already suggested in the literature based on the low temperature photon echo,[13] site-directed mutagenesis,[14] Stark spectroscopy[15] and pump–probe measurements.[48] It is most likely that the first radical pair consists of the $Chl_{D1}^{+}Pheo_{D1}^{-}$ pair.[13–15] The first charge separation generates a radical pair state of about equal energy as that of the singlet excited state of the primary electron donor. This makes recombination back to excited state highly possible. After charge recombination the excitation is equilibrated over all central chlorines in RC. This defines the blue shift (relatively to the 2–3 ps DAS) of the 30–40 ps component in fluorescence which is observed at 400, 665 and 680 nm excitation. The process of energy transfer from the peripheral Chls also contributes to this phase. It is possible that the 30–40 ps trapping phase originates from electron transfer from P_{D1} to Chl_{D1}^{+}, thus creating the $P_{D1}^{+}Pheo_{D1}^{-}$ radical pair. If this interpretation is correct, then this process would be considerably slower than in the purple bacterial RC, where this process takes place in about 3 ps. It would also mean that the 3 ps phases in the RCs of PS II and purple bacteria have different origins.

The third trapping lifetime on the 350–450 ps time scale can be interpreted by a lowering of the energy level of $P_{D1}^{+}Pheo_{D1}^{-}$ radical pair due to conformational changes of the protein surroundings. The fact that this phase, rather prominent in the time-resolved emission experiments, gives rise to only very minor absorbance changes is consistent with this idea.

5.2 CP47–RC

The data of the X-ray structures[2–4] indicate that the chlorophylls of CP47 are located at considerable distances from the chlorophylls and pheophytins of the RC. The shortest distance is 21.3 Å, between Chl43 of CP47 and $Pheo_{D2}$ of the PS II RC. This will lead to slow energy transfer between CP47 and RC, also because the excitation energy will be rapidly delocalized over the 16 Chls of CP47 and the six central Chls and Pheos of the PS II RC. Thus, one should expect to observe this component as a relatively slow phase in the time-resolved spectroscopy data.

We indeed observed slower lifetimes for the excited states decays in CP47–RC. However, the data analysis based on the kinetic model leads to the conclusion that the intrinsic time for energy transfer from CP47 to RC does not limit the trapping kinetics. According to this analysis, the upper limit for this transfer is about 20 ps. This analysis was based on the assumption that the energy levels and rate constants between the various compartments was identical for processes within the RC in the PS II RC and CP47–RC preparations. In other words, charge separation is assumed to occur in identical ways in both preparations. While there is no solid experimental evidence that would argue in favour or against this assumption, it does reflect the most simple model for charge separation in PS II.

An upper limit of about 20 ps was defined for the intrinsic time constant for energy transfer from CP47 to the RC. Only a few 'linker' chlorophylls from CP47 are directly coupled with the RC chlorines *via* energy transfer. To obtain the time constant of energy transfer between the coupled pigments the value 20 ps must be corrected for the number of Chls in CP47 and the number of 'linker' chlorophylls, which gives 2.6 ps assuming 16 Chls in CP47, two of which are 'linker' Chls. This value is of the order of the general equilibration time in the CP47 antenna. It may become slightly longer if the excited states of the 'linker' chlorophylls are populated to a larger extent than expected from a random distribution, for instance because they are red-shifted or are involved in exciton states that delocalize the main exciton state predominantly on these chlorophylls (which would also be

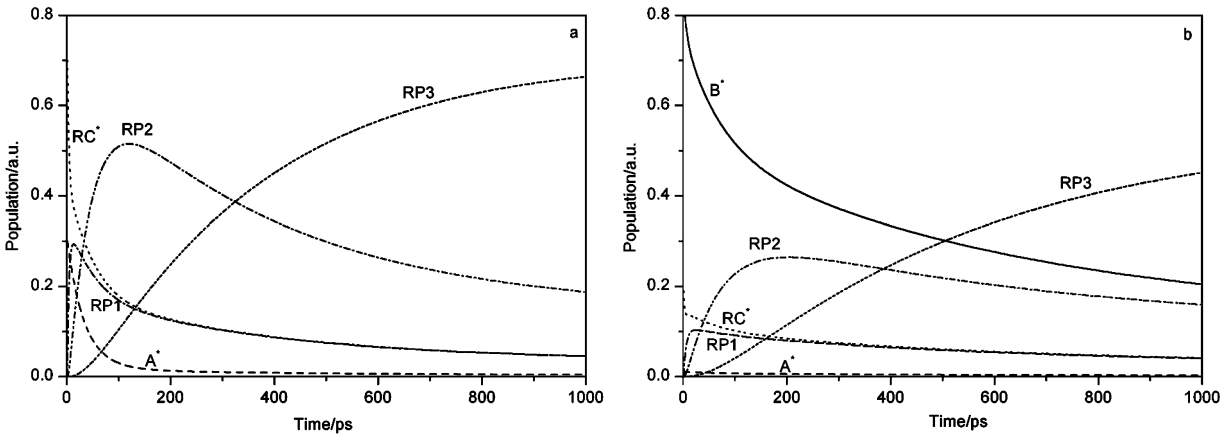

Fig. 10 Decay kinetics of the populations for each compartment of the model for the RC (a) and CP47–RC (b).

Table 2 Parameters of the model for the CP47–RC[a]

Δ_{01}/cm^{-1}	Δ_{02}/cm^{-1}	k_{01}^{-1}/ps	k_{10}^{-1}/ps	k_{02}^{-1}/ps	k_{20}^{-1}/ps
−305.5	−42.9	10	0.14	10	2

[a] The reciprocal eigenvalues: 0.14 ps; 1.3 ps; 5.8 ps; 67.2 ps; 600 ps; 12.5 ns.

caused by their relatively low site energies). According to the X-ray structures, the linker chlorophylls are ideally oriented for energy transfer to $Pheo_{D2}$,[30] supporting our conclusion about the fast rate of this process.

We calculated the difference between energy transfer rates from the nearest linker chl of CP47 (Chl43) to $Pheo_{D2}$, and from $ChlZ_{D2}$ to $Pheo_{D2}$, based on the Förster formula. The shorter distance and the more favorable orientation of the first pair of molecules suggests a ten times faster energy transfer rate from Chl43 to $Pheo_{D2}$, in agreement with the parameters of our model. We note, however, that local differences in refractive index can have a significant influence on these rates.[49,50]

Because the charge separation in the RC is highly reversible and the rate of excitation equilibration between CP47 and the RC is fast, the excited states of the CP47 antenna remain populated all the time the excitation occurs in the CP47–RC complex. The spectral properties of the CP47 antenna are also very important. The fact that the average energy level of CP47 is lower than that of the RC helps to distribute the excited states towards the core antenna.

We have found that the intrinsic rate constant of energy transfer is of the same order as the initial rate of charge separation. These results indicate that energy transfer and trapping in CP47–RC is not transfer-to-the-trap limited, as it is in the purple bacterial RC-LH1 complex.[51] However, it is also not really trap-limited, because some of the energy transfer processes occur on the same timescale, or are even slower than that of the primary charge separation reaction.

5.3 The role of CP47 antenna

A unique property of Photosystem II is that it has a high oxidation potential. It would be reasonable to assume that to prevent oxidation of the antenna components and leaking away of the positive charge from the site of water oxidation, these components must be located at long distances from the RC. The available structural data have shown that the CP47 chlorophylls are indeed located at distances of 21 Å or more. Our analysis, however, has shown that this does not prevent a fast excitation energy transfer between CP47 and RC, highlighting the light-harvesting function of CP47. It is also clear that CP47 does not play a direct role in the stabilization of the charge separation. Crucial roles in the charge stabilization are currently explained by electron transfer, in the 20–30 ps time range, from P_{D1} to Chl_{D1}^{+} and by conformational changes, in about 300 ps, of the charged protein surroundings.

At high light intensities, the rate of photosynthetic electron transport reaches a maximum. This leads to changes in the PS II antenna system which ultimately give rise to a strongly increased decay of excited states *via* internal conversion into heat by a process known as non-photochemical quenching[52] and by photodestruction of the D1 protein of the PS II RC.[53] Our results indicate that CP47 reduces the apparent rate constant of charge separation and acts as a temporary excitation storage system. The excited levels of CP47 gradually contribute to the ingrowth of radical pair populations. It is likely that the other PS II antenna complexes play similar roles. So, the fast rate constant of energy transfer between CP47 and RC helps to keep the excitation energy in the antenna system and the possibility to regulate the light need for PS II by means of the antenna. This means that the antenna has a dual function: (1) it increases the absorption cross-section, *i.e.* it increases the amount of collected light; and (2) it reduces the oversaturation of energy transfer chain.

We remark that these properties are not unique for PS II. It was shown recently that the additional IsiA antenna attached to iron-stressed cyanobacterial PS I performs similar functions: an increase of the light-harvesting capacity of PS I,[54,55] and at the same time photoprotection for PS II.[56]

Acknowledgements

We thank Henny van Roon and Marta Germano for the expert preparation of the CP47–RC and RC particles and Sandrine d'Haene for the chromatographic test of samples before and after measurement. This research was supported by the Netherlands Foundation for Scientific Research (NWO) *via* the Foundation for Life and Earth Sciences (ALW).

References

1 H. van Amerongen and J. P. Dekker, in *Light-Harvesting in Photosynthesis*, ed. B. R. Green and W. W. Parson, Kluwer Academic Publishers, Dordrecht, 2003, p. 219.
2 A. Zouni, H. T. Witt, J. Kern, P. Fromme, N. Krauß, W. Saenger and P. Orth, *Nature*, 2001, **409**, 739.
3 N. Kamiya and J.-R. Shen, *Proc. Natl. Acad. Sci. USA*, 2003, **100**, 98.
4 K. N. Ferreira, T. M. Iverson, K. Maghlaoui, J. Barber and S. Iwata, *Science*, 2004, **303**, 1831.
5 J. Barber, *Q. Rev. Biophys.*, 2003, **36**, 71.
6 A. Telfer, *Philos. Trans. R. Soc. London, Ser. B*, 2002, **357**, 1431.
7 J. P. Dekker, N. R. Bowlby and C. F. Yocum, *FEBS Lett.*, 1989, **254**, 150.
8 J. P. Dekker and R. van Grondelle, *Photosynth. Res.*, 2000, **63**, 195.
9 B. A. Diner and F. Rappaport, *Annu. Rev. Plant Biol.*, 2002, **53**, 551.
10 S. A. P. Merry, S. Kumazaki, Y. Tachibana, D. M. Joseph, G. Porter, K. Yoshihara, J. Barber, J. R. Durrant and D. Klug, *J. Phys. Chem.*, 1996, **100**, 10469.
11 M.-L. Groot, F. Van Mourik, C. Eijckelhoff, I. H. M. Van Stokkum, J. P. Dekker and R. Van Grondelle, *Proc. Natl. Acad. Sci. USA*, 1997, **94**, 4389.
12 J. R. Durrant, D. R. Klug, S. L. S. Kwa, R. van Grondelle, G. Porter and J. P. Dekker, *Proc. Natl. Acad. Sci. USA*, 1995, **92**, 4798.
13 V. I. Prokhorenko and A. R. Holzwarth, *J. Phys. Chem. B*, 2000, **104**, 11563.
14 B. A. Diner, E. Schlodder, P. J. Nixon, W. J. Coleman, F. Rappaport, J. Lavergne, W. F. J. Vermaas and D. A. Chisholm, *Biochemistry*, 2001, **40**, 9265.
15 R. N. Frese, M. Germano, F. L. de Weerd, I. H. M. van Stokkum, A. Y. Shkuropatov, V. A. Shuvalov, H. J. van Gorkom, R. van Grondelle and J. P. Dekker, *Biochemistry*, 2003, **42**, 9205.
16 S. R. Greenfield, M. Seibert, A. Govindjee and M. R. Wasielewski, *J. Phys. Chem. B*, 1997, **101**, 2251.
17 J. P. M. Schelvis, P. I. van Noort, T. J. Aartsma and H. J. van Gorkom, *Biochim. Biophys. Acta*, 1993, **1184**, 242.
18 M. G. Müller, M. Hucke, M. Reus and A. R. Holzwarth, *J. Phys. Chem.*, 1996, **100**, 9527.
19 L. M. C. Barter, J. R. Durrant and D. R. Klug, *Proc. Natl. Acad. Sci. USA*, 2003, **100**, 946.
20 T. Renger and R. A. Marcus, *J. Phys. Chem. B*, 2002, **106**, 1809.
21 G. H. Schatz, H. Brock and A. R. Holzwarth, *Biophys. J.*, 1988, **54**, 397.
22 S. A. P. Merry, P. J. Nixon, L. M. C. Barter, M. Schilstra, G. Porter, J. Barber, J. R. Durrant and D. Klug, *Biochemistry*, 1998, **37**, 17439.
23 L. Konermann, G. Gatzen and A. R. Holzwarth, *J. Phys. Chem.B*, 1997, **101**, 2933.
24 F. L. de Weerd, I. H. M. van Stokkum, H. van Amerongen, J. P. Dekker and R. van Grondelle, *Biophys. J.*, 2002, **82**, 1586.
25 F. L. de Weerd, M. A. Palacios, E. G. Andrizhiyevskaya, J. P. Dekker and R. van Grondelle, *Biochemistry*, 2002, **41**, 15224.
26 R. van Grondelle, *Biochim. Biophys. Acta*, 1985, **811**, 147.
27 A. Freiberg, K. Timpmann, A. A. Moskalenko and N. Y. Kuznetsova, *Biochim. Biophys. Acta*, 1993, **1184**, 45.

 This journal is © The Owner Societies 2004

28 L. M. C. Barter, M. Bianchietti, C. Jeans, C. Schilstra, M. J. Hankamer, B. Diner, B. A. Barber, J. R. Durrant and D. R. Klug, *Biochemistry*, 2001, **40**, 4026.
29 S. Vasil'ev, P. Orth, A. Zouni, T. G. Owens and D. Bruce, *Proc. Natl. Acad. Sci. USA*, 2001, **98**, 8602.
30 S. Vasil'ev, J.-R. Shen, N. Kamiya and D. Bruce, *FEBS Lett*., 2004, **561**, 111.
31 D. A. Berthold, G. T. Babcock and C. F. Yocum, *FEBS Lett*., 1981, **420**, 171.
32 P. J. van Leeuwen, M. C. Nieveen, E. J. van de Meent, J. P. Dekker and H. J. van Gorkom, *Photosynth. Res*., 1991, **28**, 149.
33 C. Eijckelhoff, H. van Roon, M.-L. Groot, R. van Grondelle and J. P. Dekker, *Biochemistry*, 1996, **35**, 12864.
34 C. C. Gradinaru, I. H. M. van Stokkum, A. A. Pascal, R. van Grondelle and H. van Amerongen, *J. Phys. Chem. B*, 2000, **104**, 9330.
35 I. H. M. van Stokkum, T. Scherer, A. M. Brouwer and J. W. Verhoeven, *J. Phys. Chem*., 1994, **98**, 852.
36 C. H. B. Cruz, J. P. Gordon, P. C. Becker, R. L. Fork and C. V. Shank, *IEEE J. Quantum Electron*., 1988, **24**, 261.
37 R. Monshouwer, A. Baltushka, F. van Mourik and R. van Grondelle, *J. Phys. Chem. A*, 1998, **102**, 4360.
38 B. Gobets, I. H. M. van Stokkum, M. Rogner, J. Kruip, E. Schlodder, N. V. Karapetyan, J. P. Dekker and R. van Grondelle, *Biophys. J*., 2001, **81**, 407.
39 C. Eijckelhoff, F. Vacha, R. van Grondelle, J. P. Dekker and J. Barber, *Biochim. Biophys. Acta*, 1997, **1318**, 266.
40 M. Germano, A. Ya. Shkuropatov, H. Permentier, R. de Wijn, A. J. Hoff, V. A. Shuvalov and H. J. van Gorkom, *Biochemistry*, 2001, **40**, 11472.
41 M. E. van Brederode, F. van Mourik, I. H. M. van Stokkum, M. R. Jones and R. van Grondelle, *Proc. Natl. Acad. Sci. USA*, 1999, **96**, 2054.
42 R. V. Danielius, K. Satoh, P. J. M. van Kan, J. J. Plijter, A. M. Nuijs and H. J. van Gorkom, *FEBS Lett*., 1987, **213**, 241.
43 J. P. Booth, B. Crystall, L. B. Giorgi, J. Barber, D. R. Klug and G. Porter, *Biochim. Biophys. Acta*, 1990, **1016**, 141.
44 M.-L. Groot, E. J. G. Peterman, I. H. M. van Stokkum, J. P. Dekker and R. van Grondelle, *Biophys. J*., 1995, **68**, 281.
45 M.-L. Groot, E. J. G. Peterman, P. J. M. van Kan, I. H. M. van Stokkum, J. P. Dekker and R. van Grondelle, *Biophys. J*., 1994, **67**, 318.
46 M. Volk, M. Gilbert, G. Rousseau, M. Richter, A. Ogrodnik and M.-E. Michel-Beyerle, *FEBS Lett*., 1993, **336**, 357.
47 S. Vassiliev, Ch.-I. Lee, G. W. Brudwig and D. Bruce, *Biochemistry*, 2002, **41**, 12236.
48 M. Germano, C. C. Gradinaru, A. Ya. Shkuropatov, I. H. M. Van Stokkum, V. A. Shuvalov, J. P. Dekker, R. Van Grondelle and H. J. Van Gorkom, *Biophys. J*., 2004, **86**, 1664.
49 R. S. Knox and H. van Amerongen, *J. Phys. Chem. B*, 2002, **106**, 5289.
50 M. A. Steffen, K. Lao and S. G. Boxer, *Science*, 1994, **264**, 810.
51 L. M. P. Beekman, F. Van Mourik, M. R. Jones, H. M. Visser, C. N. Hunter and R. Van Grondelle, *Biochemistry*, 1984, **33**(11), 3143.
52 P. Horton, A. V. Ruban and R. G. Walters, *Annu. Rev. Plant Physiol. Plant Mol. Biol*., 1996, **47**, 655.
53 J. Barber and B. Anderson, *Trends Biochem. Sci*., 1992, **17**, 61.
54 E. G. Andrizhiyevskaya, D. Frolov, R. van Grondelle and J. P. Dekker, *Biochim. Biophys. Acta*, 2004, **1656**, 104.
55 A. N. Melkozernov, T. S. Bibby, S. Lin, J. Barber and R. E. Blankenship, *Biochemistry*, 2003, **42**, 3893.
56 N. Yeremenko, R. Kouril, J. A. Ihalainen, S. D'Haene, N. van Oosterwijk, E. G. Andrizhiyevskaya, W. Keegstra, H. L. Dekker, M. Hagemann, E. J. Boekema, H. C. P. Matthijs and J. P. Dekker, *Biochemistry*, 2004, **43**, 10308.